Supporting Information

Ultrafast formation of an FeOOH electrocatalyst on Ni for efficient alkaline water and urea oxidation

Jun-Jun Zhang[a]*, Wei-Wei Bao[b]*, Meng-Yang Li[a], Chun-Ming Yang [c], Nan-Nan Zhang[d]

[a]School of Materials Science and Chemical Engineering, Xi'an Technological University, Xi'an, Shaanxi 710021, China.

[b]National & Local Joint Engineering Laboratory for Slag Comprehensive Utilization and Environmental Technology, School of Material Science and Engineering, Shaanxi University of Technology, Hanzhong 723000, Shaanxi, China

[c]College of Chemistry & Chemical Engineering, Yan'an University, Shaanxi Key Laboratory of Chemical Reaction Engineering, Yan'an 716000, China

[d]Instrumental Analysis Center, Shanghai Jiao Tong University, Shanghai 200240, China

Correspondence to:
E-mail: zhangjunjun@xatu.edu.cn (J. J. Zhang);
E-mail: baowei1834@163.com (W. W. B).

List of Contents

1. Experimental Section:

1.1.   Materials

1.2.   Preparation of Ni/FeOOH electrode

1.3.   Preparation of Ni + FeOOH electrode

1.4.   Preparation of IrO$_2$ electrode

1.5   Material characterizations

1.6   Electrochemical characterizations

2. Supplementary Figures:

Fig.S1. The XPS spectra of FeOOH sample.

Fig. S2. The EDS of FeOOH sample.

Fig. S3. The mass activity curves synthesized Ni/FeOOH under 1M KOH and 1M KOH+0.5M urea electrolytic system.

Fig.S4. The OER (a) Polarization curves and (b) Nyquist plots of synthesized Ni/FeOOH and bare Ni foam in 1M KOH electrolytic system.

Fig. S5. The UOR (a) Polarization curves and (b) Nyquist plots of synthesized Ni/FeOOH and bare Ni foam in 1M KOH+0.5M urea electrolytic system.

Fig. S6. The OER (a) Polarization curves and (b) Nyquist plots of synthesized Ni/FeOOH and IrO2 samples in 1M KOH electrolytic system.

Fig. S7. The UOR (a) Polarization curves and (b) Nyquist plots of synthesized Ni/FeOOH and IrO2 samples in 1M KOH+0.5M urea electrolytic system.

Fig. S8. The parameter of Nyquist plots for UOR and OER of Ni/FeOOH electrodes.

Fig. S9. the Nyquist plots of Ni/FeOOH electrode recorded at open-circuit voltage with a frequency range of 100 kHz to 0.1 Hz in UOR process under different conditions .

Fig. S10. the LSV curves recorded for Ni/FeOOH electrode before and after 500CV under UOR process.

Fig. S11. the Nyquist plots of Ni/FeOOH electrode recorded at open-circuit voltage with a frequency range of 100 kHz to 0.1 Hz in UOR process.

Fig. S12. The HR-TEM of Ni/FeOOH electrodes after stability test .

Fig. S13. The high-resolution XPS Fe 2p (a, c) and O 1s (b, d) spectra of Ni/FeOOH electrode before and after OER.

Fig. S14. The parameter of Nyquist plots for UOR of Ni/FeOOH-x (x= 5, 10, 20) electrodes.

Fig. S15. The HER (a) iR-corrected Polarization curves and (b) Nyquist plots of synthesized Ni/FeOOH samples in 1.0 M KOH and 1.0 M KOH+0.5M urea electrolytic system. (c) Polarization curves of Ni/FeOOH electrode for overall water splitting and urea electolysis (inset shows a schematic diagram of the urea electolysis). (d) time-dependent current density curve of Ni/FeOOH samples(1.6V).

Fig. S16. The Nyquist plots for urea and water electrolysis of Ni/FeOOH electrodes.

Fig. S17. The polarization curves for OER (1 M KOH) of Ni/FeOOH and counterpart Ni+FeOOH electrodes.

Fig. S18. TOF curves of Ni/FeOOH hybrid electrode, Ni+FeOOH, commercial IrO$_2$ sample.

Fig.S19. (a) the long-time i-t curves of Ni+FeOOH hybrid electrode for UOR under a constant potential. (b) polarization curves and (c) Nyquist plots before and after i-t test for UOR of Ni+FeOOH sample.

Fig. S20. CV curves of Ni+FeOOH electrodes at different scan rates from 20 to 100 mV s-1.

3.Supplementary Tables:

Table S1. Summarized the relevant synthesis parameters of Ni/FeOOH-x (x=5 , 10 , 20) hybrid electrodes.

Table S2. The comparison of UOR catalytic performance for Ni/FeOOH-x (x=5 , 10 , 20) electrocatalysts.

Table S3. The Comparison of the OER performance of NF/FeOOH catalyst with other reported OER catalysts

Table S4: The comparison of the UOR performance of NF/FeOOH catalyst with other reported UOR catalysts.

4.   Notes and references

1. Experimental Section

1.1 Materials

Sodium nitrate ($NaNO_3$), hexahydrate ferric chloride ($FeCl3·6H2O$), ruthenium dioxide (RuO_2), and Nafion (5 wt%) were purchased from Shinopharm Chemical Reagent Co., Ltd. Milli-Q ultrapure water was used for all experiments. Nickel foam (NF) were used as the substrate. All chemicals were used as received without further purification.

1.2. Preparation of Ni/FeOOH electrode

Prior to the reaction, nickel (Ni) foam was firstly washed with HCl solution under ultrasonic for 20 min, ethanol and water several times to remove the surface impurities and to ensure a clean surface. For a typical run, sodium nitrate (1270mg) and hexahydrate ferric chloride (608mg) were dissolved in water (25 mL) at 100 ℃ for 8 min. Then, the as-made Ni foam was immersed into the heated solution (10s). The resulting Ni/FeOOH was then washed with ethanol and further dried at ambient temperature. The loading amount of the catalysts was 0.53 mg cm^{-2}. In addition, a series of Ni/FeOOH-x (x=5, 10, 20; immersed time) products were also synthesized for different loading of the FeOOH. Relevant synthesis parameters was listed in Table S1.

1.3. Preparation of Ni + FeOOH electrode

To prepare FeOOH loaded electrodes, 2 mg FeOOH and 20 μL 5 wt% Nafion solution were dispersed in 0.2 mL 3:7 water/ethanol solvent. The mixture was ultrasonicated for about 2 h to form a homogeneous ink. Then, 58 μL catalyst ink was loaded on a preprocessed Ni foam (1*1 cm^2). The loading amount of the catalysts was 0.53 mg cm^{-2}.

1.4. Preparation of IrO$_2$ electrode

To prepare IrO_2 loaded electrodes, 2 mg IrO_2 and 20 μL 5 wt% Nafion solution were dispersed in 0.2 mL 3:7 water/ethanol solvent. The mixture was ultrasonicated for about 2 h to form a homogeneous ink. Then, 58 μL catalyst ink was loaded on a preprocessed Ni foam (1*1 cm^2).

1.5 Material characterizations

The X-ray diffraction (XRD) patterns were recorded on a Bruker D8 Advance X-ray diffractometer with Cu-Kα radiation (λ = 1.5418 Å) with a scan rate of 6° min^{-1}. The SEM measurements were performed on ascanning electron microscope (FESEM, JSM-7610F, 10 kV). The TEM and HRTEM measurements were taken with a JEOL JEM-F200 microscope operated. The X-ray photoelectron spectroscopy (XPS) measurements were conducted on a Kratos Axis Ultra DLD spectrometer. The ICP measurements were conducted on a Perkin-Elmer Optima 3300DV ICP spectrometer for the loading analysis.

1.6 Electrochemical characterizations

Electrochemical measurements are performed with a CHI 730C electrochemistry workstation (CH Instruments, Inc., Shanghai) in a standard three-electrode system. The three-electrode electrochemical cell was consisted of a Ni/FeOOH, a graphite carbon rod and a mercury oxide electrode (Hg/HgO) served as working electrode, counter electrode, and reference electrode, respectively. Potentials are reported versus the reversible hydrogen electrode (RHE). All potentials were calculated with respect to RHE via the following equation: $E_{RHE} = E_{Hg/HgO} + 0.059pH + 0.098$ V. Polarization curves measurements were conducted in 1.0 M KOH and 1.0 M KOH + 0.5 M urea solution with a scan rate of 5 mV s^{-1}. All the polarization curves are the steady-state ones after several cycles. The long-term durability test was performed using chronoamperometric measurements. The cyclic voltammogram (CV) 500 cycles durability test was conducted by potential cycling from 0.2 to 1.8 V vs. RHE. The scan rate for cycling was fixed at 50 mV s^{-1}. Double layer capacitance measurements were conducted by varying the scan rates (20-100 mV s^{-1} with an interval 20 mV) in a potential window nearly without Faradaic process. The plot of the current density under a set overpotential vs. scan rates has a linear relationship, and its slope is the double layer capacitance. The polarization curves were establish as overpotential vs log current (log j) to get Tafel plots for evaluating the OER reaction kinetics of obtained catalysts. By fitting the Tafel plots (the linear portion) to the Tafel equation ($\eta = blog(j) + a$), the Tafel slope can be obtained. To reflect the real catalytic currents, all corresponding polarization curves shown in this paper were calibrated after i*Rs correction. E corrected = E measured − i*Rs (where Ecorr is the i*Rs-compensated potential, Emea is the experimentally measured potential, and Rs is the solution resistance, respectively). Electrochemical impedance spectroscopy (EIS) is a common method for investigating the as-constructed electron transfer kinetics in the OER and UOR process. The EIS measurements for the Ni/FeOOH were performed in 1.0 M KOH and 1.0 M KOH + 0.5 M urea solution at a bias voltage of 0.6 V vs. (Hg/HgO) using a graphite rod as the counter electrode with the frequency range from 100 KHz to 0.1 Hz. The turnover frequency (TOF) is defined as the number of H_2 or O_2 molecules generated per site per second: $TOF = j/(n*F*N)$, where j is the measured current density (A cm^{-2}), n is the mole number of electrons per mole of O_2, F is the Faraday constant (96485 C mol^{-1}), and N is the content of the catalyst (mol cm^{-2}). All measurements were conducted at room temperature.

2. Supplementary Figures:

Fig. S1. The XPS spectra of FeOOH sample.

Fig. S2. The EDS of FeOOH sample.

Fig. S3. The mass activity curves synthesized Ni/FeOOH under 1M KOH and 1M KOH + 0.5M urea electrolytic system.

Fig.S4. The OER (a) Polarization curves and (b) Nyquist plots without fitting of synthesized Ni/FeOOH and bare Ni foam in 1M KOH electrolytic system.

Fig. S5. The UOR (a) Polarization curves and (b) Nyquist plots without fitting of synthesized Ni/FeOOH and bare Ni foam in 1M KOH+0.5M urea electrolytic system.

Fig. S6. The OER (a) Polarization curves and (b) Nyquist plots without fitting of synthesized Ni/FeOOH and IrO$_2$ samples in 1M KOH electrolytic system.

Fig. S7. The UOR (a) Polarization curves and (b) Nyquist plots without fitting of synthesized Ni/FeOOH and IrO₂ samples in 1M KOH + 0.5M urea electrolytic system.

Fig. S8. The parameter of Nyquist plots for UOR and OER of Ni/FeOOH electrodes.

Fig. S9. the Nyquist plots without fitting of Ni/FeOOH electrode recorded at open-circuit voltage with a frequency range of 100 kHz to 0.1 Hz in UOR process under different conditions (0.5-0.8V).

Fig. S10. the LSV curves recorded for Ni/FeOOH electrode before and after 500CV under UOR process.
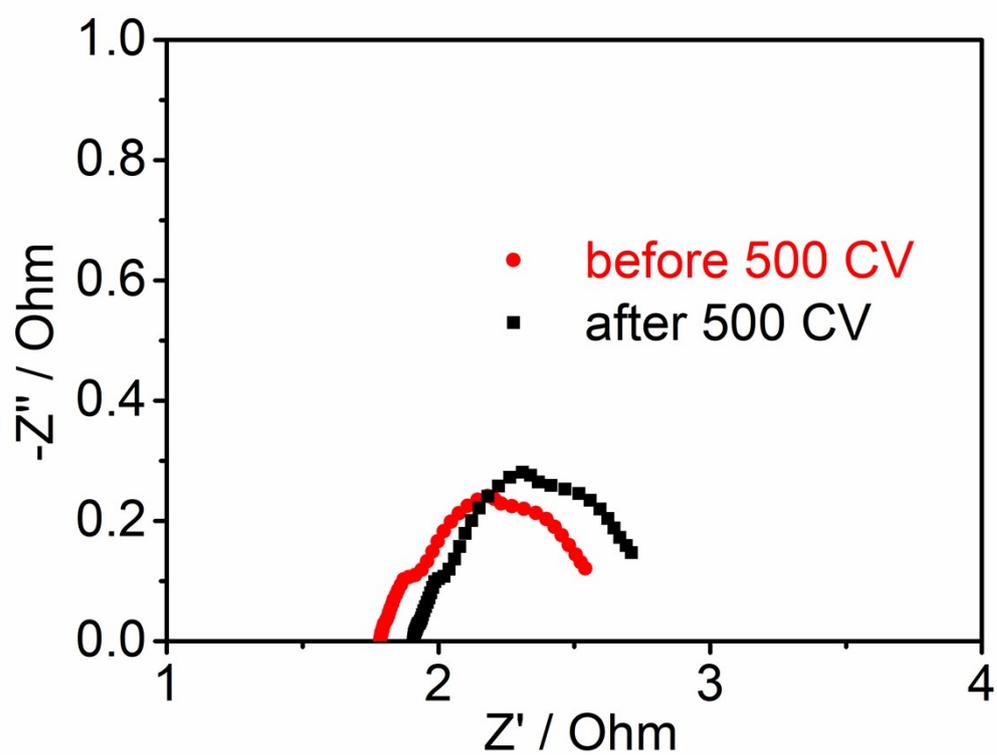
Fig. S11. the Nyquist plots without fittingof Ni/FeOOH electrode recorded at open-circuit voltage with a frequency range of 100 kHz to 0.1 Hz in UOR process.
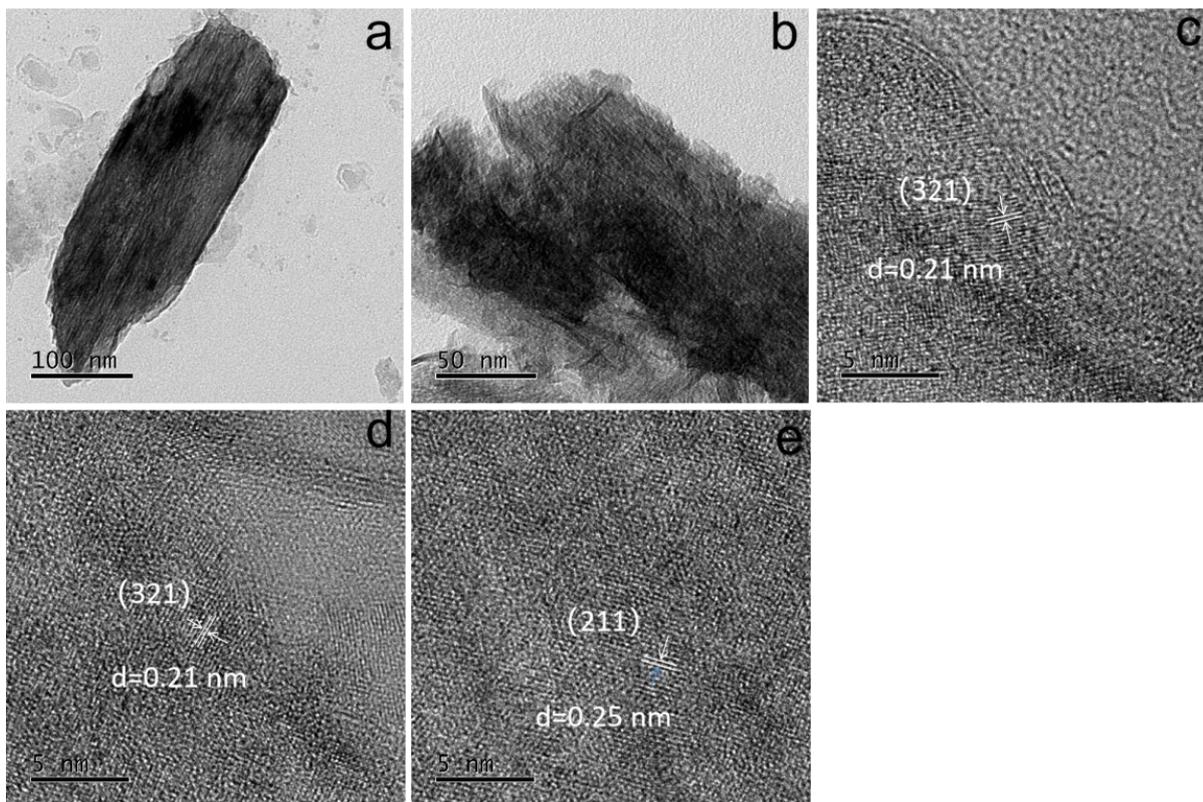
Fig. S12. The HR-TEM of Ni/FeOOH electrodes after stability test .
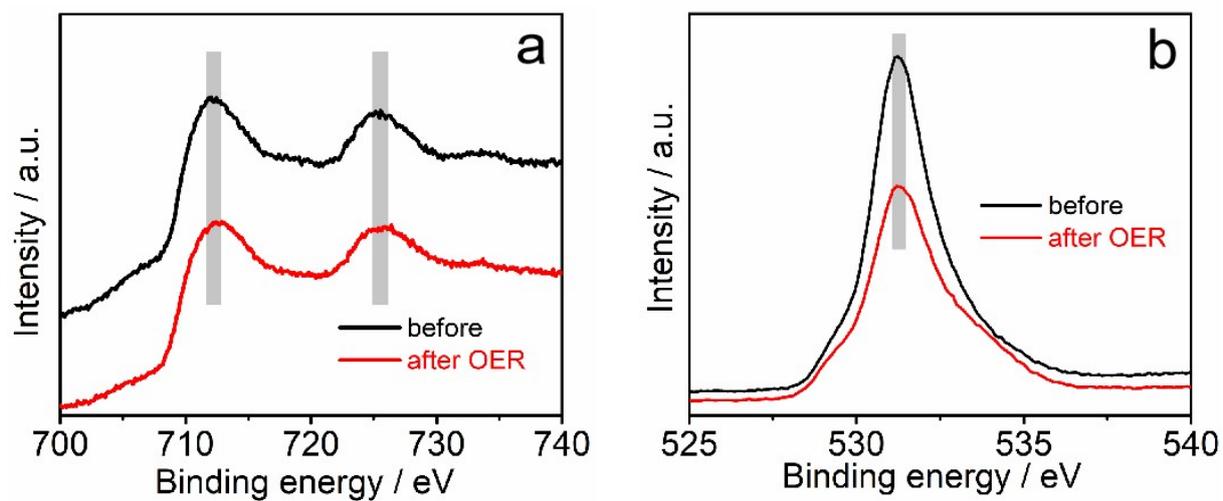
Fig. S13. The high-resolution XPS Fe 2p (a) and O 1s (b) spectra of Ni/FeOOH electrode before and after OER.
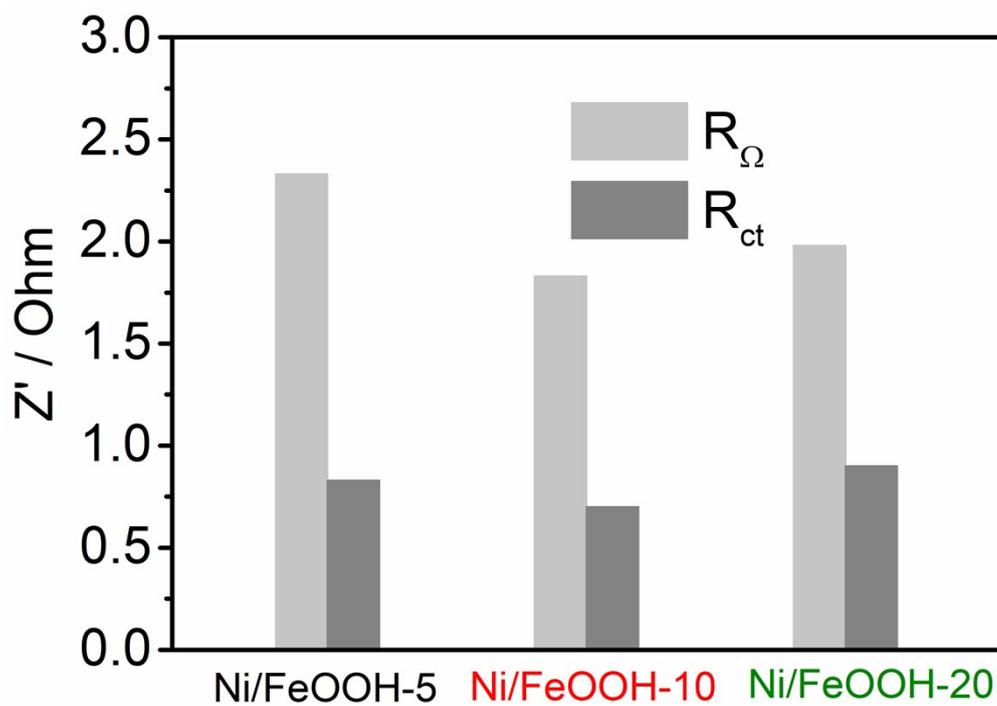
Fig. S14. The parameter of Nyquist plots for UOR of Ni/FeOOH-x (x= 5, 10, 20) electrodes.

Fig. S15. The HER (a) iR-corrected Polarization curves and (b) Nyquist plots of synthesized Ni/FeOOH samples in 1.0 M KOH and 1.0 M KOH+0.5M urea electrolytic system. (c) Polarization curves of Ni/FeOOH electrode for overall water splitting and urea electolysis (inset shows a schematic diagram of the urea electolysis). (d) time-dependent current density curve of Ni/FeOOH samples(1.6V).
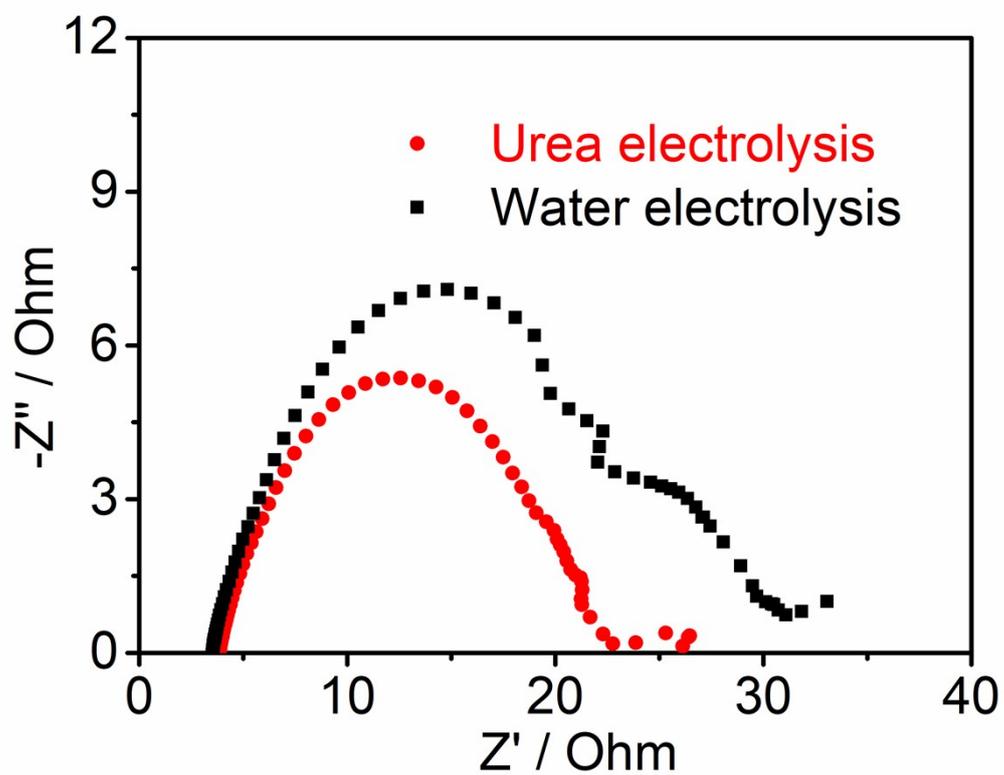
Fig. S16. The Nyquist plots without fitting for urea and water electrolysis of Ni/FeOOH electrodes.
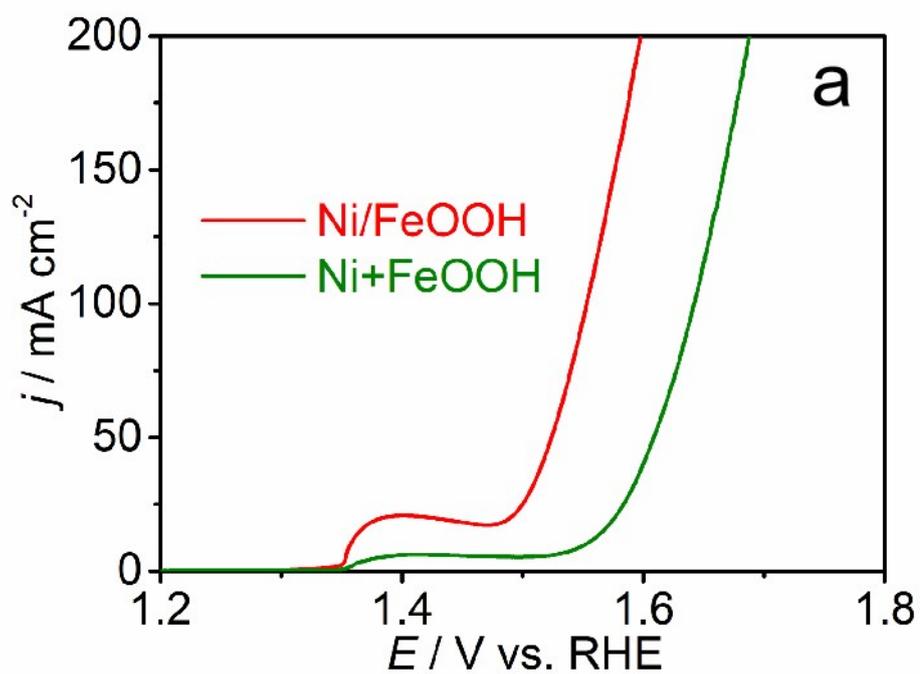
Fig. S17. The Polarization curvesr OER (1 M KOH) of Ni/FeOOH and counterpart Ni+FeOOH electrodes.
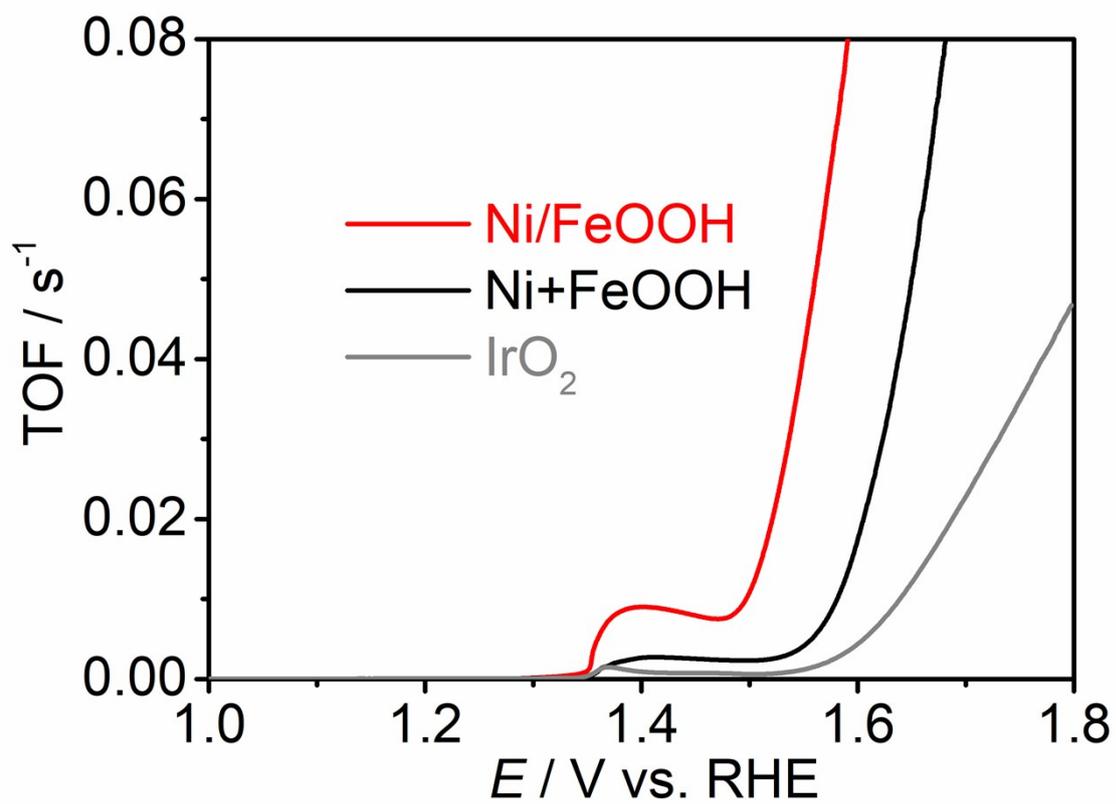
Fig. S18. TOF curves of Ni/FeOOH hybrid electrode, Ni+FeOOH, commercial IrO_2 sample.
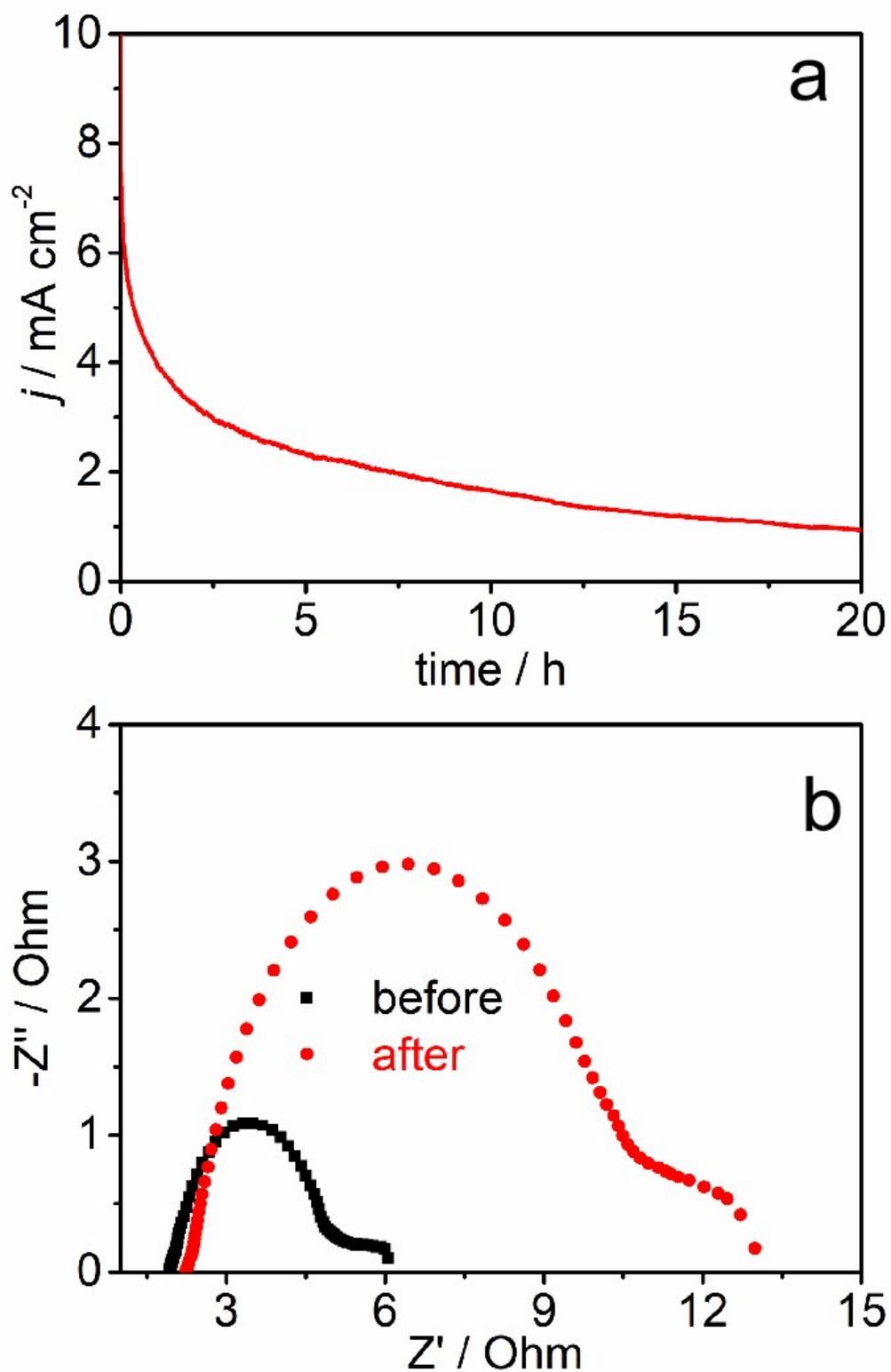
Fig. S19. (a) the long-time i-t curves of Ni+FeOOH hybrid electrode for UOR under a constant potential. (b) Nyquist plots without fitting before and after i-t test for UOR of Ni+FeOOH sample.
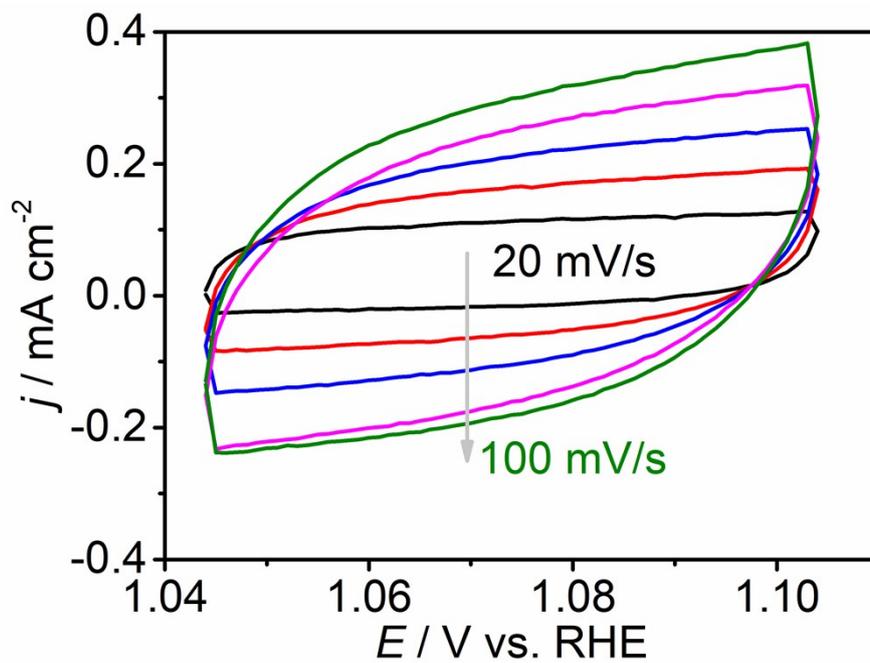
Fig. S20. CV curves of Ni+FeOOH electrodes at different scan rates from 20 to 100 mV s-1.

3.   Supplementary Tables

Table S1. Summarized the relevant synthesis parameters of Ni/FeOOH-x (x=5 , 10 , 20) hybrid electrodes.

Samples	$NaNO_3$(mg)	$FeCl_3$.(mg)	H_2O (mL)	Time (s)
Ni/FeOOH-5	1270	608	30	5
Ni/FeOOH-10	1270	608	30	10
Ni/FeOOH-20	1270	608	30	20

Table S2. Comparison of UOR catalytic performance for Ni/FeOOH-x (x=5 , 10 , 20) electrocatalysts.

Catalysts	E @ 100 mA cm^{-2}
Ni/FeOOH-5	1.449
Ni/FeOOH-10	1.407
Ni/FeOOH-20	1.473

Table S3. Comparison of the OER performance of Ni/FeOOH catalyst with other reported OER catalysts

Catalyst	Loading/mg	Tafel slope (mV dec-1)	j (mA cm-2)	E/ V vs. RHE	Reference
Ni/FeOOH	0.53	97	50	1.52	This work
CC/CoO	0.19	44	10	1.56	1.Nat. Commun., 2016, 7, 12876.
Fe(OH)$_3$:Cu(OH)$_2$	2.8	42	10	1.59	2.ChemComm, 2016,52, 14470-14473
Fe-CoOOH/G	0.20	37	10	1.56	3.Adv. Energy Mater. 2017, 1602148
NiCo$_2$S$_4$ nanowire	Not give	40.1	10	1.57	4.Adv. Funct. Mater. 2016, 26, 4661
CoMnP	0.284	61	10	1.56	5.J. Am. Chem. Soc, 2016, 138, 4006-4009
NF/Ni@Mo$_2$C-PC	2.0	150	10	1.53	6.Chem. Sci., 2017, 8, 968-973.
CoTe NR/NF	1.3	75	100	1.58	7.Small Methods 2019, 3, 1970013
Ni$_3$S$_2$/AT-Ni	Not give	163	10	1.547	8.Electrochimica Acta 174 (2015) 297–301
NiCo$_2$O4 hollow microcuboids	1.0	53	10	1.52	9.Angew. Chem. Int. Ed. 2016, 55, 6290 –6294
Au-Ir	20 μg cm^{-2}	36.9	10	1.475	10.Nature Communications，2020，DOI: 10.1038/s41467-020-15391-w
CoOOH NS	0.15	38	10	1.53	11.Angew. Chem. Int. Ed. 2015, 54, 8722 –8727
NF@Co-HNNs	Not give	170	10	1.555	12. ChemElectroChem,2019,62050-2055
FeOOH2 nm/LDH	0.25	35	50	1.48	13.ACS Catal. 2018, 8, 11342−11351
Co$_2$Mo$_3$O$_8$	0.14	87.5	10	1.561	14.Angew. Chem. Int. Ed. 2020, DOI: 10.1002/anie.202004533
Ni-Doped AlOOH	Not give	Not give	10	1.55	15.ACS Sustainable Chem. Eng. 2019, 7, 5953−5962
Cu foil/Co$_3$O$_4$-C	0.2	70	10	1.52	16.J. Am. Chem. Soc., 2014, 136, 13925-13931
CVN/CC	2.0	64.1	10	1.557	17.Applied Catalysis B: Environmental 241 (2019) 521–527
VOOH	0.8	68	50	1.55	18.Angew. Chem. 2017, 129, 588 –592, DOI: 10.1002/anie.201610211
FeOOH	Not give	Not give	7	1.8	19.J. Mater. Chem. A, 2017,5, 2021-2028
Au foil/CoP/PO$_4$	Not give	65	30	1.56	20.Adv. Mater., 2015, 27, 3175-3180.

Table S4: Comparison of the UOR performance of NF/FeOOH catalyst with other reported UOR catalysts.

Catalyst	Loaging/mg	Tafel slope (mV dec-1)	j (mA cm^{-2})	E / V vs. RHE	Reference
Ni/FeOOH	**0.53**	**26**	**10**	**1.373**	**This work**
	0.53	**26**	**50**	**1.393**	
	0.53	**26**	**100**	**1.407**	
	0.53	**26**	**200**	**1.427**	
NF/NiMoO-Ar	4.5	19	100	1.42	21.Energy Environ. Sci., 2018, 11, 1890-1897. DOI: 10.1039/C8EE00521D
NF/MnO2	1.5	75	100	1.45	22.Angew. Chem. Int. Ed, 2016, 55, 3804-3808
Ni$_2$P/CFC	Not give	78	50	1.55	23.Electrochem. Acta, 2017, 254, 44-49.
NiCo alloy	1.0	Not give	10	1. 5	24.Sci. Rep., 2014, 4, 5863
HC-NiMoS	1.42	19.2	60	1.39	25.Nano Research, 2018,11, 988-996
Ni(OH)$_2$	0.535	Not give	10	1.42	26.Angew. Chem. Int. Ed., 2016, 55, 12465-12469
NF-Pt/C	1.5	105	10	1.48	27.Angew. Chem. Int. Ed, 2016, 55, 3804-3808
Rh-Ni	Not give	Not give	30	1.58	28.J. Power sources , 2011, 196, 9579-9584
Ni(OH)$_2$-graphene	Not give	Not give	10	1.43	29.Electrochem. Acta, 2013, 89, 732-736.
Ni-Co	0.67	Not give	30	1.6	30.Electrochem. Acta 2012, 61, 25–30
Ni wires	1.3	Not give	30	1.51	31.Electrochem. Acta 2014, 134, 266–271

4. Notes and references

[1] Tao Ling, Dong-Yang Yan, Yan Jiao, Hui Wang, Yao Zheng, Xueli Zheng, Jing Mao, Xi-Wen Du, Zhenpeng Hu, Mietek Jaroniec & Shi-Zhang Qiao, *Nat. Commun.*, **2016**, 7, 12876.

[2] Chun-Chao Hou, Chuan-Jun Wang, Qian-Qian Chen, Xiao-Jun Lv, Wen-Fu Fu and Yong Chen, *Chem. Commun.* **2016**, 52, 14470-14473.

[3] Han, Xiaotong, Yu, Chang, Qiu, Jieshan, *Adv. Energy Mater.* **2017**, 7, 1602148.

[4] A. Sivanantham, Pandian Ganesan, Sangaraju Shanmugam, *Adv. Funct. Mater.* **2016**, 26, 4661-4672.

[5] Li, D, Baydoun, Habi; Verani, CN, Brock, Stephanie L, *.J. Am. Chem. Soc,* **2016**, 138, 4006-4009.

[6] Zi-You Yu, Yu Duan, Min-Rui Gao, Chao-Chao Lang, Ya-Rong Zheng and Shu-Hong Yu, *Chem. Sci.,* **2017,**8, 968-973.

[7] Liu Yang, Haoxiang Xu, Huibing Liu, Daojian Cheng Dapeng Cao, *Small Methods* **2019**, 3, 1900113.

[8] Canbin Ouyang, Xin Wang, Chen Wang, Xiaoxu Zhang, Jianghong Wu, Zhaoling Ma, Shuo Dou, Shuangyin Wang, *Electrochimica Acta*, **2015**, 174, 297-301.

[9] Xuehui Gao, Hongxiu Zhang, Quanguo Li, Xuegong Yu, Zhanglian Hong, Xingwang Zhang, Chengdu Liang, Zhan Lin, *Angew. Chem. Int. Ed.* **2016**, 55, 6290 –6294.

[10] Ran Du, Jinying Wang, Ying Wang, René Hübner, Xuelin Fan, Irena Senkovska, Yue Hu,

 Stefan Kaskel & Alexander Eychmüller,, *Nat. Commu*，**2020**，11, 1590

[11] Junheng Huang, Junting Chen, Tao Yao, Jingfu He, Shan Jiang, Zhihu Sun, Qinghua Liu, Weiren Cheng, Fengchun Hu, Yong Jiang, Zhiyun Pan, Shiqiang Wei, *Angew. Chem. Int. Ed.* **2015**, 54, 8722 –8727

[12] Mingyang Yang, Xuelian Fu, Mengmeng Shao, Zhenyu Wang, Lujie Cao, Shuai Gu, Minchan Li, Hua Cheng, Yuchao Li, Hui Pan, Zhouguang Lu, *ChemElectroChem*, **2019**, 62050-2055,

[13] Jiande Chen, Feng Zheng, Shao-Jian Zhang, Adrian Fisher, Yao Zhou, Zeyu Wang, Yuyang Li, Bin-Bin Xu, Jun-Tao Li, Shi-Gang Sun, *ACS Catal.* **2018**, 8, 11342-11351.

[14] Zhao-Qing Liu Ting Ouyang Xiao-Tong Wang Xiu-Qiong Mai An-Na Chen Zi-Yuan Tang, *Angew. Chem. Int. Ed.* **2020**, 59, 11948-11957.

[15] Zhou, Yao, Zeng, Hua Chun, *ACS Sustainable Chem. Eng.* **2019**, 7, 5953−5962.

[16] Tian Yi Ma, Sheng Dai, Mietek Jaroniec, Shi Zhang Qiao, *J. Am. Chem. Soc.* **2014**, 136, 39, 13925-13931.

[17] Soumen Dutta, Arindam Indra, Yi Feng, HyukSu Han, Taeseup Song, *Applied Catalysis B: Environmental,* **2019***,* 241, 521–527.

[18] Huanhuan Shi, Hanfeng Liang, Fangwang Ming, Zhoucheng Wang, *Angew. Chem. Int. Ed. ,* **2017**, 56, 573-577.

[19] Wenjun Luo, Chaoran Jiang, Yaomin Li, Stephen A. Shevlin, Xiaoyu Han, Kaipei Qiu, Yingchun Cheng, Zhengxiao Guo, Wei Huang and Junwang Tang, *J. Mater. Chem. A*, **2017**,5, 2021-2028.

[20] Yang Yang, Huilong Fei, Gedeng Ruan, James M. Tour, *Adv. Mater.*, **2015**, 27, 3175-3180

[21] Zi-You Yu, Chao-Chao Lang, Min-Rui Gao, Yu Chen, Qi-Qi Fu, Yu Duan and Shu-Hong Yu, *Energy Environ. Sci.*, **2018,** 11, 1890-1897.

[22] Sheng Chen, Jingjing Duan, Anthony Vasileff, Shi Zhang Qiao, *Angew. Chem. Int. Ed,* **2016**, 55, 3804-3808.

[23] Xian Zhang, YanyanLiu, QizhongXiong, GuoqiangLiu, CuijiaoZhao, Guozhong Wang, Yunxia Zhang, HaiminZhang, HuijunZhao, *Electrochem. Acta*, **2017**, 254, 44-49.

[24] Wei Xu, Huimin Zhang, Gang Li, Zucheng Wu, *Scientific Reports*, **2015**, 4, 5863.

[25] Xiaoxia Wang, Jianmei Wang, Xuping Sun, Shuang Wei, Liang Cui, Wenrong Yang & Jingquan Liu, *Nano Research*, **2018**, 11, 988–996.

[26] Xiaojiao Zhu, Xinyu Dou, Jun Dai, Xingda An, Yuqiao Guo, Lidong Zhang, Shi Tao, Jiyin Zhao, Wangsheng Chu, Xiao Cheng, Changzheng Wu, Yi Xie, *Angew. Chem. Int. Ed.*, **2016**, 55, 12465-12469.

[27] Sheng Chen, Jingjing Duan, Anthony Vasileff, Shi Zhang Qiao, *Angew. Chem. Int. Ed,* **2016**, 55, 3804-3808.

[28] Rebecca L.King, Gerardine G.Botte, *J. Power sources*, **2011**, 196, 9579-9584,

[29] D. Wang, W. Yan, S. H. Vijapur, G. G. Botte, Electrochim. Acta 2013, 89, 732-736;

[30] Wei Yan, Dan Wang, Gerardine G. Botte, *Electrochem. Acta* **2012**, 61, 25–30,

[31] Wei Yan, Dan Wang, Luis A. Diaz, Gerardine G. Botte, *Electrochem. Acta* **2014**, 134, 266–271,